SANDIA REPORT

SAND90—2619 • UC—814
Unlimited Release
Printed July 1991

Yucca Mountain Site Characterization Project

Dual Porosity Models for Solute Transport at Yucca Mountain

R. C. Dykhuizen

Prepared by
Sandia National Laboratories
Albuquerque, New Mexico 87185 and Livermore, California 94550
for the United States Department of Energy
under Contract DE-AC04-76DP00789

HYDROLOGY DOCUMENT NUMBER 661

SF2900Q(8-81)

"Prepared by Yucca Mountain Site Characterization Project (YMSCP) participants as part of the Civilian Radioactive Waste Management Program (CRWM). The YMSCP is managed by the Yucca Mountain Project Office of the U.S. Department of Energy, Nevada Operations Office (DOE/NV). YMSCP work is sponsored by the Office of Geologic Repositories (OGR) of the DOE Office of Civilian Radioactive Waste Management (OCRWM)."

Issued by Sandia National Laboratories, operated for the United States Department of Energy by Sandia Corporation.

NOTICE: This report was prepared as an account of work sponsored by an agency of the United States Government. Neither the United States Government nor any agency thereof, nor any of their employees, nor any of their contractors, subcontractors, or their employees, makes any warranty, express or implied, or assumes any legal liability or responsibility for the accuracy, completeness, or usefulness of any information, apparatus, product, or process disclosed, or represents that its use would not infringe privately owned rights. Reference herein to any specific commercial product, process, or service by trade name, trademark, manufacturer, or otherwise, does not necessarily constitute or imply its endorsement, recommendation, or favoring by the United States Government, any agency thereof or any of their contractors or subcontractors. The views and opinions expressed herein do not necessarily state or reflect those of the United States Government, any agency thereof or any of their contractors.

Printed in the United States of America. This report has been reproduced directly from the best available copy.

Available to DOE and DOE contractors from
Office of Scientific and Technical Information
PO Box 62
Oak Ridge, TN 37831

Prices available from (615) 576-8401, FTS 626-8401

Available to the public from
National Technical Information Service
US Department of Commerce
5285 Port Royal Rd
Springfield, VA 22161

NTIS price codes
Printed copy: A03
Microfiche copy: A01

SAND90-2619
Unlimited Release
Printed July 1991

Distribution
Category UC-814

Dual Porosity Models for Solute Transport at Yucca Mountain

R. C. Dykhuizen
Thermal and Fluid Engineering Division
Sandia National Laboratories
Albuquerque, New Mexico 87185

Abstract

A fractured porous medium is often modeled as a dual porosity system. The subsystems of fractures and matrix pores are assumed to provide two flow continuums. This is especially true when considering solute transport through such a system. Coupling terms are then required to enable the calculation of the exchange of solute between the two subsystems. The coupling terms for solute transport through a fractured medium are derived in this report. This report then investigates the need for the dual porosity models for solute transport. It is shown that the complexity of a dual porosity model is required in some cases to accurately represent the solute motion. However, it is also shown that some situations can be well represented by approximate single porosity models if certain criteria are met. A single porosity model allows the use of analytical solutions. Sample calculations are presented using parameter values representative of Yucca Mountain tuffs. These calculations show that a dual porosity model is not required to model solute transport at Yucca Mountain if the water fluxes are as low as currently believed.

Contents

1 INTRODUCTION 5
2 DEVELOPMENT OF A DUAL POROSITY MODEL 6
3 COUPLING TERMS 7
3.1 Coupling Term Derivation 8
3.2 Coupling Term Demonstration 11
3.3 Discussion of the Coupling Term 14
3.4 Conclusions for the Coupling Term 14
4 MOMENT ANALYSIS 15
4.1 Derivation of the Moments 16
4.2 Discussion of the Moment Analysis 21
4.3 Verification of the Moment Analysis 22
4.4 Conclusions for the Moment Analysis 27
5 SAMPLE CALCULATIONS USING YUCCA MOUNTAIN PROPERTIES . 28
6 CONCLUSIONS 32
7 REFERENCES 34
Appendix A. Reference Information Base 37

1 INTRODUCTION

A dual porosity model includes two flow fields through the porous medium. In regions with significant fracture flow, the solute can bypass much of the retention capabilities of the matrix pore system. This can result in solute traveling faster than the average water velocity (based upon the total porosity).

The earliest dual porosity (or dual velocity) models were introduced in the field of chemical engineering (Lapidus and Amundson, 1952; Glueckauf, 1955). These models described the transport of ions in ion exchange columns. The ions may reside in one of two systems. The first is the flowing fluid, and the second is the ion exchange resin (typically a non-flowing system of spherical beads). Coupling terms are proposed for the exchange of ions between the two systems.

A second dual porosity model is the dead-end pore model for solute transport in geologic media (Deans, 1963; Coats and Smith, 1964). In this model the pore space of a geologic medium is divided into two distinct sets. The first set is interconnected and contains a flowing fluid. This fluid exchanges solute with a stagnant fluid contained in a second set of pores (dead-end pores).

Of most importance to the Yucca Mountain Project is a dual porosity system that represents a fractured porous medium. This was first analyzed by Barenblatt, *et al.* (1960) and Warren and Root (1963). In these models a liquid saturated, fractured, geologic system is analyzed. The fracture system provides a transport path for the solute. The matrix pores of the rock between the fractures is modeled as a (typically) non-flowing system that can remove (or replenish) solute from the fracture system. This type of model can be extended to a partially liquid-saturated, fractured medium if the liquid in the matrix pore system is allowed to have a convective velocity (Dykhuizen, 1987). Further studies on saturated systems have been performed by numerous authors (*e.g.*, Fogden *et al.*, 1988; Grisak and Pickens, 1980; Neretnieks and Rasmuson, 1984).

Pigford *et al.* (1980) introduced a model to describe the non-equilibrium sorption of solutes onto a geologic medium. This is not usually considered a dual porosity system, but may be cast into that general form. One system is the flowing fluid, which interacts with a non-flowing medium. Solute may reside in the flowing fluid, or be fixed on the non-flowing medium. Typically, a proportionality constant (k_d) is used to describe the mass balance of the solute in the two systems. The introduction of a time constant to describe the approach to this equilibrium yields the dual porosity model equations. This non-zero time constant could be due to a slow surface reaction rate, or due to the diffusion of the solute to a discrete set of locally reactive minerals (Casey, 1987; Rubin, 1983).

Zanotti and Carbonell (1984a) introduce a model of two-phase flow in a geologic medium. In this model both subsystems have a non-zero velocity. The solute may reside in both of the phases. Again, an equilibrium constant is introduced to describe the

equilibrium partition of the solute between the phases. A time constant is introduced to describe the approach to equilibrium.

2 DEVELOPMENT OF A DUAL POROSITY MODEL

The following are the governing equations solved for the dual porosity model of a fractured system (presented in a single dimension for simplicity):

$$(\theta_m + \rho_s k_d)\frac{\partial C_m}{\partial t} + v_m \frac{\partial C_m}{\partial z} - \frac{\partial}{\partial z}\left[D_m \frac{\partial C_m}{\partial z}\right] = -W(C_x - C_m) + \Psi - \lambda(\theta_m + \rho_s k_d) C_m \ , \tag{1}$$

$$\theta_f \frac{\partial C_f}{\partial t} + v_f \frac{\partial C_f}{\partial z} - \frac{\partial}{\partial z}\left[D_f \frac{\partial C_f}{\partial z}\right] = +W(C_x - C_f) - \Psi - \lambda \theta_f C_f \ , \tag{2}$$

where

- C_m is the matrix pore solute concentration,
- C_f is the fracture solute concentration,
- C_x is the cross flow solute concentration,
- D is the diffusion/dispersion coefficient,
- k_d is the distribution coefficient,
- v is the infiltration flux (positive downward),
- W is the cross flow rate,
- z is the coordinate in the flow direction,
- λ is the radioactive decay constant,
- θ is the moisture content,
- ρ_s is the bulk rock density, and
- Ψ is the cross diffusion rate.

In the above, it is assumed that the solute is not retarded while flowing through the fracture subsystem. However, if data are available, this can easily be included. Note that the model of retardation assumes that chemical equilibrium is instantly obtained between the sorbed and dissolved states of the solute.

The sub-model for Ψ is described in Section 3. This accounts for the diffusional exchange of solute between the two flow systems.

A model was constructed to obtain the diffusion/dispersion coefficient. This model is presented by Freeze and Cherry (1979).

$$D = \frac{\theta D^*}{\tau} + \alpha v \ , \tag{3}$$

where

τ is the tortuosity,
α is the dispersivity, and
D^* is the molecular diffusion coefficient of the solute in water.

The tortuosity is often considered to be a function of the saturation level of the geologic material, with increasing tortuosity resulting from a decrease in the moisture content. A model from Burdine (1953) was used to describe this effect,

$$\tau = \frac{\tau_s}{\left[\frac{(S-S_r)}{(1-S_r)}\right]^2}, \tag{4}$$

where

τ_s is the saturated tortuosity,
S is the saturation level, and
S_r is the residual saturation level.

In this model for solute transport the microscopic wetted surface of the porous material is assumed to be independent of the saturation level. This needs to be established from experiments. However, the assumption results in a distribution coefficient (k_d) that is independent of the saturation level.

The cross flow solute concentration (C_x, which is used in the advection between the two subsystems) is determined from the direction of the flow between the two subsystems. The advected flow rate (W') is obtained from a simple mass balance. The cross flow submodel is presented in Dykhuizen (1987).

3 COUPLING TERMS

To close the dual porosity model presented above the coupling term needs to be evaluated. In this section a model for the coupling term is developed. This model is based upon the work presented in Dykhuizen (1990). Most models initially consider a system of parallel fractures that align with the flow direction (Figure 1). A tortuosity factor must be included in the fracture flow equations when the fractures are not parallel or aligned with the flow direction. Unequal spacing of the fractures needs to be considered, although it will be assumed here that a single representative fracture spacing is suitable.

The dual porosity solute transport equation set is repeated here. The solute is assumed to be stable, so the decay term is deleted. The overbar placed over the matrix concentration is to emphasize that this concentration is an average over the matrix pore block between fractures. No such distinction is made for the fracture flow system because

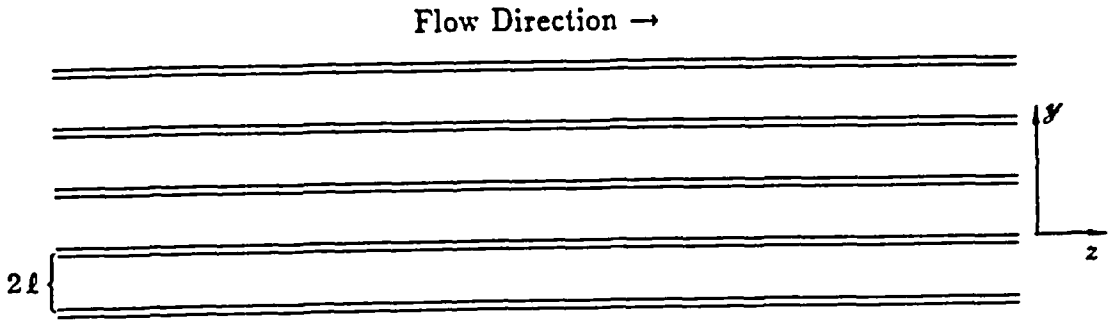

Figure 1. Simplistic parallel fracture geometry.

the fractures are typically so narrow, and diffusion so rapid, that the local value is very close to the average value:

$$(\theta_m + \rho_s k_d)\frac{\partial \overline{C_m}}{\partial t} + v_m \frac{\partial \overline{C_m}}{\partial z} - \frac{\partial}{\partial z}\left[D_m \frac{\partial \overline{C_m}}{\partial z}\right] = -W\left(C_x - \overline{C_m}\right) + \Psi \ , \tag{5}$$

$$\theta_f \frac{\partial C_f}{\partial t} + v_f \frac{\partial C_f}{\partial z} - \frac{\partial}{\partial z}\left[D_f \frac{\partial C_f}{\partial z}\right] = +W\left(C_x - C_f\right) - \Psi \ . \tag{6}$$

The integral approximation method will be used to derive the coupling term. Classical works providing foundations for the integral approximation are found in Pohlhausen (1921) and Goodman (1964). Later classic applications of this method include Eckert and Drake (1986) and Schlichting (1968). A recent paper Zimmerman and Bodvarsson (1989) uses the integral method to calculate unsaturated flows of fluid in a porous medium.

3.1 Coupling Term Derivation

In implementing this method, it is assumed that the fractures form a parallel set of planes in the direction of the flow, and the existence of perpendicular fractures does not affect the results. It is further assumed that the flow conditions are such that the flow in the matrix pores is negligible compared to the flow in the fractures. Also, the transport of solute in the matrix pores is primarily perpendicular to the fractures.

A submodel for the matrix pores between the fractures is now considered. For the above assumptions, the following equation applies in the matrix pores where the fractures are in planes of constant y and the flow is in the z direction:

$$(\theta_m + \rho_s k_d)\frac{d}{dt}\int_o^\ell C_m(z,y,t)dy = \frac{\theta_m D^*}{\tau_m}\frac{\partial C_m}{\partial y}\Big|_\ell \ , \tag{7}$$

where $y = 0$ is midway between fractures, and 2ℓ is the fracture spacing. The overbar does not appear in Equation 7 since the matrix concentration is not averaged over the volume between the fractures here. The left hand side of Equation 7 represents the rate of increase in the solute content in the matrix pore system. This is set equal to the incoming flux of solute at the fracture surface.

In the above equation, a concentration profile in the matrix pore system must be assumed. The accuracy of the solution is strongly affected by the accuracy of the assumed profiles. In this section, two separate profiles will be used: one will be used for early times and one for late times. This division is not arbitrary, and justifications will be offered for both the choice of the functional form and switch-over time. The late time solution derivation will be shown first, because its choice determines many of the parameters for the early time solution.

First assume that the fluid concentration in the fractures which surround the matrix pore system is a known function of time. (The coupling of the two systems will be presented later.) Because the fluid concentration will be continuous, the matrix pore fluid concentration at the fracture edge ($y = \ell$) will be the same as the fracture fluid concentration:

$$C_m(z, \ell, t) = C_f(z, t) \ . \tag{8}$$

Assuming that the fracture fluid concentration varies smoothly and monotonically at large values of time, the fundamental mode of the matrix solution will be dominant (Carslaw and Jaeger, 1978). The fundamental mode is the one with the largest time constant. Therefore, the following functional form is proposed:

$$C_m(z, y, t) = (C_f(z, t) - C_{mo}) \left[1 - f(z, t) \cos \frac{\pi y}{2\ell}\right] + C_{mo} \ , \tag{9}$$

where $f(z, t)$ is function of time and position, and C_{mo} is an assumed constant initial matrix concentration level. It will be shown that the function $f(z, t)$ will not have to be determined, for it will be eliminated via the integral method.

Using Equation 9, Equation 7 becomes

$$\frac{d\overline{C_m}}{dt} = \frac{\theta_m D^* \pi}{\tau_m(\theta_m + \rho_s k_d) 2\ell^2} f(x, t) \left[C_f(y, t) - C_{mo}\right] \ , \tag{10}$$

where $$\overline{C_m}(y, t) = \frac{1}{\ell} \int_o^\ell C_m(z, y, t) dy \ . \tag{11}$$

Using Equations 9 and 11 to relate $f(z,t)$ to the mean matrix and fracture system fluid concentrations the following is obtained:

$$\overline{C_m} = C_f - [C_f(y,t) - C_{mo}] \frac{2f(z,t)}{\pi} . \tag{12}$$

Equation 12 is used to eliminate the function $f(x,t)$ in Equation 10. This yields the governing equation for large times,

$$\frac{d\overline{C_m}}{dt} = \frac{\theta_m D^*/\tau_m}{\theta_m + \rho_s k_d} \left(\frac{\pi}{2\ell}\right)^2 (C_f(y,t) - \overline{C_m}(y,t)) . \tag{13}$$

Equation 13 was also derived by Laplace transform methods (Wilson and Dudley, 1987) or series expansion (Dykhuizen, 1987) for the quasi-steady approximation.

It is desired to match the above solution, which is appropriate for late times, to a solution that will yield accurate simulations for early times. Obviously, at early times the assumed profile (Equation 9) does not apply. In fact, a boundary layer is formed that travels from the fracture towards the center of the matrix block. Therefore, the following profile will be assumed:

$$\begin{aligned} C_m(z,y,t) &= C_{mo} + (C_f(x,t) - C_{mo}) \left[1 - \cos \frac{\pi(y - \delta(z,t))}{2(\ell - \delta(z,t))}\right] \quad \text{for } y > \delta(z,t) \\ C_m(z,y,t) &= C_{mo} \qquad \text{for } y < \delta(z,t) , \end{aligned} \tag{14}$$

where δ represents the distance to the boundary layer from the center of the matrix block. Initially δ would be equal to ℓ (the half fracture spacing).

Using Equations 7 and 11 in a manner similar to that above, the governing equation for early times is obtained:

$$\frac{d\overline{C_m}}{dt} = \frac{\theta_m D^*/\tau_m}{\theta_m + \rho_s k_d} \left[\frac{C_f(z,t)}{\ell}\right]^2 \frac{(\pi/2 - 1)}{\overline{C_m}(z,t)} . \tag{15}$$

The choice of the switch-over time now becomes clear. When the boundary layer is equal to the half fracture spacing the two profiles will be identical ($f(z,t)$ will be unity at the transition and $\delta(z,t)$ will be zero). This condition makes the numerical value of the coupling term the same, since the flux at the boundary will be identical. This continuity will assure a smooth transition. The condition can be found by using the transition profile in Equation 11 to obtain the following:

$$\overline{C_m}(z,t) = [C_f(z,t) - C_{mo}](1 - 2/\pi) + C_{mo} \,. \tag{16}$$

3.2 Coupling Term Demonstration

Before using this model to simulate a coupled transient flow in a fractured porous medium, some simple test problems were computed to evaluate how this model compares to the quasi-steady model. To accomplish this, a non-dimensional time is introduced,

$$\Upsilon = \frac{\theta_m D^* \, t}{\tau_m(\theta_m + \rho_s k_d)\ell^2} \,. \tag{17}$$

Two test problems were run. The first shows the response of the average matrix fluid concentration to a step change in the fracture fluid concentration. Figure 2 shows a comparison of the exact solution, the quasi-steady solution, and the new model presented here. As shown, the new model results in a significant improvement. The new model resulted in a switch-over from the early (high) coupling term to the quasi-steady coupling term at a non-dimensional time of 0.23. The switchover yields a smooth transition, and no discontinuity in either the value or the slope of the matrix concentration results.

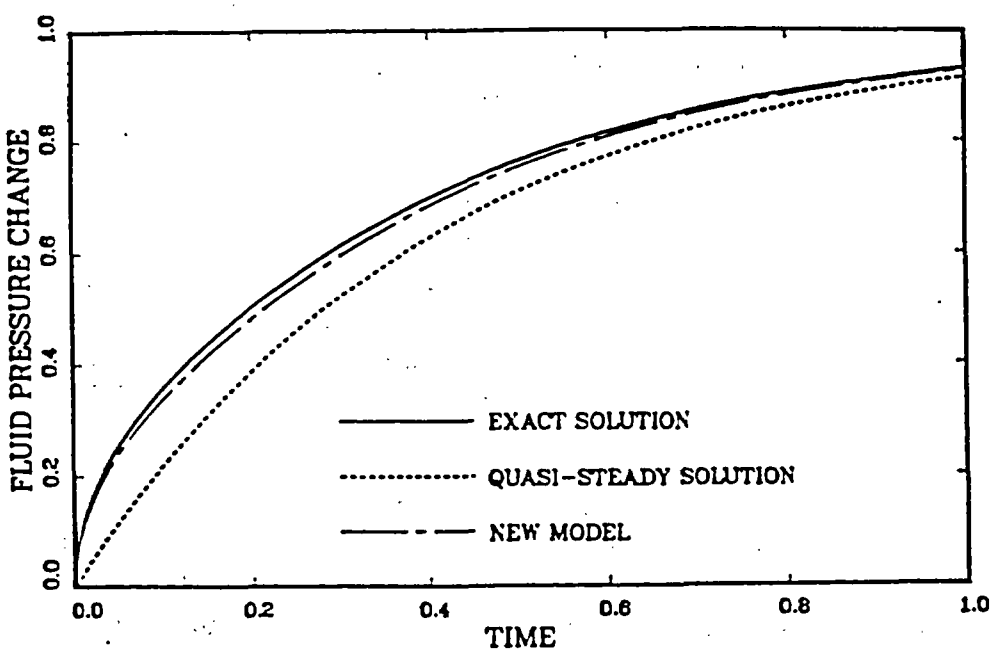

Figure 2. Comparison of models for a step change in the fracture fluid concentration. (Time non-dimensionalized via Equation 17.)

The second test is to calculate an example problem where the two solute concentrations are actually coupled. The following equation set is postulated here to simulate

solute transport in a dual porosity medium:

$$\begin{aligned} \frac{\partial C_f}{\partial t} + \frac{v_f}{\theta_f}\frac{\partial C_f}{\partial z} - \frac{D_f}{\theta_f}\frac{\partial^2 C_f}{\partial z^2} &= \frac{-\Psi}{\theta_f}, \\ \frac{\partial \overline{C_m}}{\partial t} &= \frac{\Psi}{\theta_m}. \end{aligned} \tag{18}$$

The model for the coupling term is obtained from Equation 15 for early times and Equation 13 for late times. Therefore, using the above definitions for conductivities and capacitances, the following is obtained:

$$\begin{aligned} \Psi &= \frac{\theta_m D^* (\pi/2 - 1) C_f^2}{\tau_m \ell^2 \overline{C_m}} \quad \text{if } \overline{C_m} < C_f(1 - 2/\pi), \\ \Psi &= \frac{\theta_m D^* \pi^2}{2\tau_m \ell^2}(C_f - \overline{C_m}) \quad \text{if } \overline{C_m} > C_f(1 - 2/\pi). \end{aligned} \tag{19}$$

This equation set (18 and 19) will yield averaged fracture and matrix solute concentration as a function of distance and time. Note that convection and diffusion along the flow direction are assumed to be negligible in the matrix pores. For this problem, the fracture concentration is of primary interest because transport in the fractures is dominant. Therefore, the fracture concentration results will be presented.

The quasi-steady model uses the late time formulation for the coupling term at all times. At early times this approximation underestimates the extent of the coupling. In fact, in the limit of infinite fracture spacing, the coupling term goes to zero in both the fracture and the matrix governing equations. However, if the early time choice is used, the coupling remains finite in the fracture system equation. This term remains finite because the matrix concentration and the fracture porosity will both scale inversely with the fracture spacing.

The governing equations (Equation set 18) were solved numerically by the method of lines. The mesh contained 35 nodes 0.3333 cm apart. Table 1 presents the parameters used. The results from both the quasi-steady model and the new model are presented in Figure 3, as is an analytical solution to a similar problem for comparison. The analytical solution corresponds to the same equation set, except that there is no axial diffusion in the fracture flow system and it uses an infinite fracture spacing (Carslaw and Jaeger, 1978). The time in Figure 3 is scaled by the fracture travel time and is, thus, non-dimensional. The following equation defines the time scaling for Figure 3:

$$\Upsilon = \frac{v_f t}{X \theta_f}, \tag{20}$$

where X is 10 cm, the output position.

Table 1. Parameters for Calculating Example Solute Transport Problem.

V_f	=	1. E-10	m/sec
θ_f	=	1.E-4	—
θ_m	=	.1	—
D^*	=	1.E-10	m^2/sec
τ_m	=	10.	—
τ_f	=	10.	—
ℓ	=	0.075	m
α_f	=	0	m

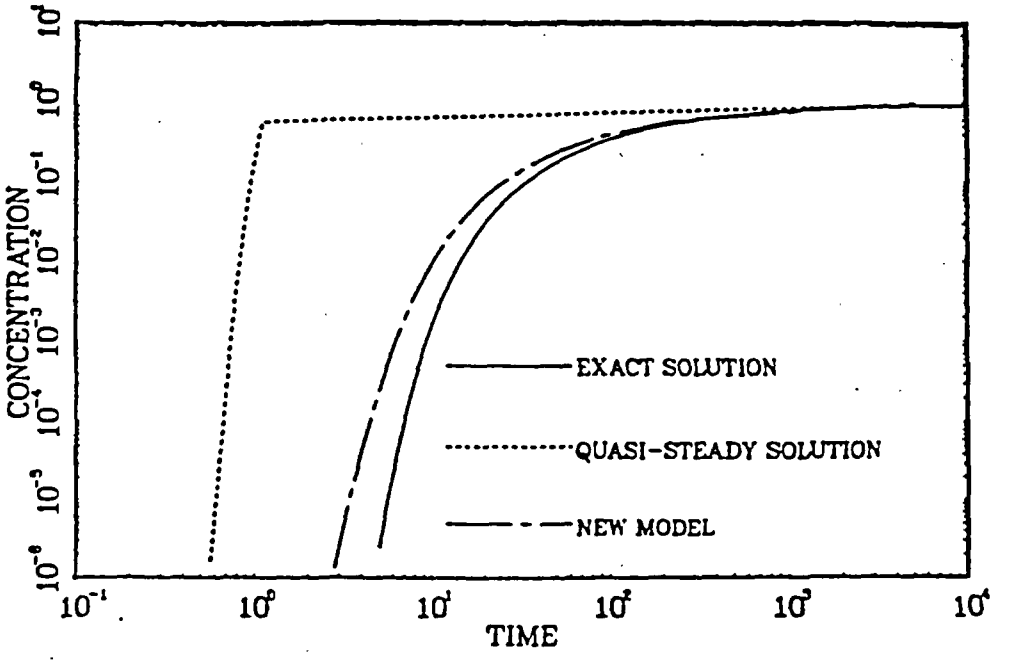

Figure 3. Comparison of breakthrough curves for 10 cm depth (fracture concentration; Time non-dimensionalized via Equation 20.)

This scaling results in the solute front arriving at the output location at a dimensionless time of unity, if the coupling is deleted from the model.

As can be seen in Figure 3, the quasi-steady model indicates little delay of the solute transport for this problem. This is because the coupling term is almost zero in the quasi-steady model of this problem. The new model provides a much better estimate of the solute transport.

3.3 Discussion of the Coupling Term

The parameters used in these calculations were chosen to illustrate the large differences between the two models. These differences arise when the quasi-steady model time-constant (see Equation 17) for diffusion into the matrix material is large (three orders of magnitude larger in this case) compared to the fracture travel time. This resulted in the new model primarily using the early time coupling term. The early time coupling is much larger and resulted in an order-of-magnitude increase in the amount of solute diffusing into the matrix pores (although the average matrix concentration still remains two orders of magnitude below the fracture concentration). Therefore the arrival of the solute is shown to be significantly delayed in the new model.

The difference between the new model and the analytical result can be attributed to four causes. The largest source of error is numerical diffusion present in the solution of the finite-differenced equations. The slope of the breakthrough curve of the new model at low concentrations is very sensitive to numerical diffusion. The calculation presented was performed with very small node spacings and central differences to minimize the effect of numerical diffusion. Other calculations with larger node spacings and upwind differences resulted in a more gradual rise in the breakthrough curve. However, the region between dimensionless concentrations of 0.1 and 1.0 was hardly affected. The second cause of a difference is the treatment of the fracture spacing. The analytical solution corresponds to a fluid flow of the same velocity as the new model but with infinite fracture spacing. Therefore, the analytic model did not include the effect of solute from a neighboring fracture. Because this does happen in the new model solution near the top of the simulation region, the new model resulted in a somewhat earlier arrival of the solute downstream. The last two causes for the differences result in relatively minor errors. The new model includes axial diffusion, which was determined to be very small in this case but was not included in the analytical solution. Finally, the approximations in the integral method result in some disagreement with the analytical solution.

It is interesting to note that this coupling term has been investigated for many years in the Chemical Engineering literature. Glueckauf (1955) reviews a series of approximate forms for the coupling term in the analysis of spherical ion-exchange-column particles. These proposed forms include one that is identical to the late time form presented here. Another one of the proposed forms for the coupling term was very similar to the early time form presented here; however, it included a second term to prevent overshoot of the equilibrium condition. It is felt that this analysis presents the first attempt at using two different forms of the coupling term to enable accurate simulation of both the early and late behavior.

3.4 Conclusions for the Coupling Term

A new model has been derived for the coupling of two flow systems in a dual porosity model. The new formulation eliminates the quasi-steady approximation in deriving

the coupling term. This approximation has been described as a major shortcoming by Berkowitz, *et al.* (1988). The only extra calculation required is a choice in the coupling term based upon a switch-over relation. This model can be used for the transport of fluid, heat or solute by simply switching the potential used in the formulation.

The model is best applied to the flow of heat or solute where the governing differential equation for the matrix submodel is linear. For the transport of heat or solute in the matrix subsystem, a linear governing differential equation is typically assumed, and therefore, the assumed profiles will be very good. The flow of groundwater in a saturated or nearly saturated medium will also be linear. However, application of this method to the nonlinear flow of a highly unsaturated medium may require different functional forms for the matrix pore system profiles, Zimmerman and Bodvarsson (1989). Also, the model relies on functional shapes that are appropriate only for monotonically varying transient concentration. Use of the model for oscillatory boundary conditions will not yield good results.

The new coupling term is nonlinear. This makes the solution somewhat more difficult than the quasi-steady model (which is linear), but numerical solutions are typically always used. Because of the decreased stiffness of the model equations, the new model can often take orders-of-magnitude less computer time for completion. Example problems were presented which show improved predictions of solute transport with the new model.

4 MOMENT ANALYSIS

In this section, asymptotic solutions are obtained for solute transport in the dual porosity system. These are obtained via the analysis of the moments of particular solutions. From this analysis, non-dimensional parameters will be found that will enable one to determine when a dual porosity model is required. In some situations the coupling is very strong, and one can assume that the matrix and fracture solute concentrations are locally in equilibrium. In some cases an asymptotic condition can be approached where an effective single continuum exists, resulting in a single system with an increased dispersion.

For the convection-diffusion equation set for two coupled pore systems, a linear coupling time constant, η, is assumed to be known from experiments, or from a more basic model. As shown in the previous section, a linear coupling term is only valid for the long time portion of the coupling. To account for the increased coupling in the earlier time of the transient, a linear coupling of increased magnitude over the long time response should be used here. Parker and Valocchi (1986) provide an excellent discussion on obtaining this time constant for a fractured system that allows preservation of the actual moments. Van Genuchten (1985) also shows a derivation of an effective linear coupling term for use over all times. This increased linear coupling is less than a factor of two over the long time linear coupling term derived in the previous section.

The governing equations presented as Equations 1 and 2 are simplified for this analysis to form the following equation set:

$$\theta_a \frac{\partial C_a}{\partial t} + v_a \frac{\partial C_a}{\partial z} - D_a \frac{\partial^2 C_a}{\partial z^2} = \frac{(C_b - C_a)}{\eta} \quad . \tag{21}$$

Because we are concerned with two interacting pore sets, there are two such equations, one for the conservation of the solute in the a set, and the other for conservation of the solute in the b set. The equations, as formulated here, are always symmetric so only the a equations will be presented. The corresponding b equation can be obtained by replacing all of the a subscripts by b, and *vice versa*.

The above assumes no advective coupling between the subsystems, and no radioactive decay. It also assumes that the saturation and material properties are homogeneous over space and time, and no sorption of the solute. Solute sorption can be included in this derivation, however, it was omitted for ease of presentation. The equations are slightly more complex when a retention coefficient is included. The fluid velocities are considered steady.

Solutions of the above equation set for arbitrary initial and boundary conditions are difficult to obtain. However, moments of the solution can be constructed and evaluated analytically. This was first done for solute transport in one-dimensional pulsed flow by Taylor (1953), and later improved upon by Aris (1956). A coated tube with solute exchange between the fluid and the coating was the first examination of a coupled system (Westhaver, 1942). Other coupled conditions were examined by Golay (1958) and Aris (1959). Zanotti and Carbonell (1984b) provide a connection between the various results of Taylor, Aris, Westhaver and Golay.

4.1 Derivation of the Moments

Various moments are derived in the following subsections. The results will yield insights into solute transport in dual porosity systems.

Zeroth Moment

The zeroth moment of a pulsed system is obtained by integrating Equation 21 over all values of z. Given that the concentrations are zero at plus and minus infinity, the following is obtained:

$$\frac{dM_{ao}}{dt} = \frac{-1}{\eta} \left(\frac{M_{ao}}{\theta_a} - \frac{M_{bo}}{\theta_b} \right) , \tag{22}$$

where

$$M_{ao} = \int_{-\infty}^{+\infty} \theta_a \, C_a \, dz \; .$$

The addition of the two zeroth moment equations (Equation 22) for the two pore sets shows that solute is conserved:

$$\frac{d(M_{ao} + M_{bo})}{dt} = 0 \; . \tag{23}$$

By dividing the zeroth moment equations by their respective porosities, and then subtracting one from the other, the following differential equation is obtained:

$$\frac{d\,(M_{ao}/\theta_a - M_{bo}/\theta_b)}{dt} = \frac{-1}{\eta} \left(\frac{\theta_a + \theta_b}{\theta_a \theta_b} \right) \left(\frac{M_{ao}}{\theta_a} - \frac{M_{bo}}{\theta_b} \right) \; . \tag{24}$$

By a simple substitution of variables,

$$\delta_o = \frac{M_{ao}}{\theta_a} - \frac{M_{bo}}{\theta_b} \; , \tag{25}$$

a single ordinary differential equation for δ_o results. A solution is easily found:

$$\delta_o = \delta_o(0) \; exp \left(- \frac{(\theta_a + \theta_b)}{\eta \theta_a \theta_b} t \right) \; . \tag{26}$$

Equation 26 indicates that, as time goes to infinity, δ_o goes to zero. So

$$\frac{M_{ao}}{\theta_a} = \frac{M_{bo}}{\theta_b} \tag{27}$$

when $t >> t_e = \dfrac{\theta_a \theta_b \eta}{(\theta_a + \theta_b)}$.

This shows that chemical equilibrium, in a global sense, is approached. However, this does not mean that local chemical equilibrium is established everywhere. Consider the case of fractured-medium flow. At the front of the flowing pulse, the solute concentration is higher in the fracture. Therefore, solute diffuses from the fractures into the rock matrix. However, after the pulse passes, the concentration is higher in the matrix pores and diffuses back into the fractures. Yet globally, the solute is distributed proportionally to the capacitance of the two systems.

When the result for δ_o is put back into the original moment Equations 22, it is shown that the zeroth moments approach a constant value for each system.

First Moment

The first moment of the solute distribution in the pulsed system yields some insight into the spatial distribution and velocity of the solute in each of the two pore sets. If Equation 21 is multiplied by z, and integrated over all z, the following equation is obtained:

$$\frac{dM_{a1}}{dt} = \frac{v_a M_{ao}}{\theta_a} - \frac{1}{\eta}\left(\frac{M_{a1}}{\theta_a} - \frac{M_{b1}}{\theta_b}\right) \quad , \tag{28}$$

where

$$M_{a1} = \int_{-\infty}^{+\infty} z\theta_a C_a dz \quad .$$

The mean position of the pulse is defined as

$$\mu_a = M_{a1}/M_{ao} \quad . \tag{29}$$

Noting that M_{ao} was determined to be a constant for large times, and is related to M_{bo} by Equation 27, the following differential equation is obtained:

$$\frac{d\mu_a}{dt} = \frac{v_a}{\theta_a} - \frac{\mu_a - \mu_b}{\theta_a \eta} \quad . \tag{30}$$

If δ_1 is defined to be the difference between the two mean positions,

$$\delta_1 = \mu_a - \mu_b \quad , \tag{31}$$

the following exponential solution is found:

$$\delta_1 = \frac{\eta(\theta_b v_a - \theta_a v_b)}{(\theta_a + \theta_b)}\left\{1 - \; exp\left[\frac{-(\theta_a + \theta_b)t}{\theta_a \theta_b \eta}\right]\right\} + \delta_1(0)\; exp\left[\frac{-(\theta_a + \theta_b)t}{\theta_a \theta_b \eta}\right] \quad . \tag{32}$$

Note that this solution has the same time constant as found for δ_o. A steady-state value for δ_1 is obtained as

$$\delta_1 = \frac{(\theta_b v_a - \theta_a v_b)\eta}{(\theta_a + \theta_b)} \quad \text{for} \quad t >> \frac{\theta_a \theta_b \eta}{(\theta_a + \theta_b)} \quad . \tag{33}$$

This solution was also found empirically through computer simulations and via a dimensional analysis for the fractured media application. Substitution of this solution (Equation 33) into the governing equations for the mean position (Equation 30) yields:

$$\frac{d\mu_a}{dt} = \frac{d\mu_b}{dt} = \frac{v_a + v_b}{\theta_a + \theta_b} \quad . \tag{34}$$

Therefore, the total volumetric flux divided by the total capacity gives the asymptotic velocity of the pulse in both pore sets. From this, we might expect that the dual velocity medium can be treated as a single effective medium at large times. We also see that for large times, the pulse in the "faster" pore set (the one with the larger value of v/θ) will lead the pulse in the "slower" pore set by a constant amount.

Second Moment

Finally, we will investigate the second moment of the pulsed system to enable calculation of the dispersion of the combined pore sets. Einstein (1905) showed that the change of the variance with respect to time yields the diffusion (or in this case the diffusion/dispersion) coefficient. The variance, of course, can be calculated from the second moment,

$$\sigma = \omega - \mu^2 \quad , \tag{35}$$

where σ is the variance and ω is the reduced second moment.

The second moment is obtained multiplying Equation 21 by z^2 and integrating over all z:

$$\frac{dM_{a2}}{dt} = \frac{2\ v_a M_{a1}}{\theta_a} + \frac{2\ D_a M_{ao}}{\theta_a} - \frac{1}{\eta}\left(\frac{M_{a2}}{\theta_a} - \frac{M_{b2}}{\theta_b}\right) \quad , \tag{36}$$

where

$$M_{a2} = \int_{-\infty}^{+\infty} z^2\ \theta_a C_a dz \quad .$$

We note here that for the pulsed system M_{ao} is constant at large times. Therefore, by dividing Equation 36 by M_{ao}, the following differential equation is obtained:

$$\frac{d\omega_a}{dt} = \frac{2\ v_a \mu_a}{\theta_a} + \frac{2\ D_a}{\theta_a} - \frac{1}{\eta}\left(\frac{\omega_a}{\theta_a} - \frac{M_{b2}}{\theta_b M_{ao}}\right) \quad , \tag{37}$$

where

$$\omega_a = M_{a2}/M_{ao} \quad .$$

Using Equation 27, which is applicable for large times, Equation 37 simplifies to

$$\frac{d\omega_a}{dt} = \frac{2\ v_a \mu_a}{\theta_a} + \frac{2\ D_a}{\theta_a} - \frac{1}{\eta}\left(\frac{\omega_a}{\theta_a} - \frac{\omega_b}{\theta_a}\right) \quad . \tag{38}$$

The time derivative of the variance is found from Equations 27, 30, 35, and 38 where, at large times,

$$\frac{d\sigma_a}{dt} = \frac{\delta_1^2}{\eta\theta_a} + \frac{2D_a}{\theta_a} - \frac{(\sigma_a - \sigma_b)}{\eta\theta_a} \quad . \tag{39}$$

From the two equations described above (one for each subsystem) the following can be formed:

$$\frac{d\delta_2}{dt} = -\frac{\delta_1^2}{\eta}\left(\frac{\theta_a - \theta_b}{\theta_a\theta_b}\right) + 2\left(\frac{D_a}{\theta_a} - \frac{D_b}{\theta_b}\right) - \left(\frac{\theta_a + \theta_b}{\theta_a\theta_b}\right)\frac{\delta_2}{\eta} \quad , \tag{40}$$

where

$$\delta_2 = \sigma_a - \sigma_b \quad .$$

Again, an exponential solution is obtained with the same time constant as before. The variable, δ_2, exponentially approaches the following steady value:

$$\delta_2 = \frac{\delta_1^2(\theta_b - \theta_a)}{\theta_a + \theta_b} + 2\eta\left(\frac{D_a\theta_b - D_b\theta_a}{\theta_a + \theta_b}\right) \quad , \tag{41}$$

when $t >> \dfrac{\theta_a\theta_b\eta}{(\theta_a + \theta_b)}$.

When this solution is substituted into Equation 39, a constant increase in the variance occurs for both pore sets. This translates to the same effective dispersion coefficient for both systems:

$$D_e = \frac{1}{2}\frac{d\sigma}{dt} = \frac{\delta_1^2/\eta + D_a + D_b}{\theta_a + \theta_b} \quad . \tag{42}$$

Here, it is seen that the coupling term adds to the effective dispersion of the combined pore sets. Solute is stored in the slower pore set, and then returns into the faster pore set after the pulse has passed. This result reduces to the same as that derived by DeSmedt and Wierenga (1984) for their special case of a dead end pore system.

4.2 Discussion of the Moment Analysis

Analysis of the moments of the solutions for the dual velocity solute transport equations has determined a very simple asymptotic behavior. For large times, the solute motion can be described by a single effective velocity and dispersion coefficient. Thus, a single governing equation can be written for the solute motion in the combined pore sets:

$$\frac{\partial C}{\partial t} + V_e \frac{\partial C}{\partial z} - D_e \frac{\partial^2 C}{\partial z^2} = 0 \ , \tag{43}$$

where

$$V_e = \frac{v_a + v_b}{\theta_a + \theta_b} \ , \quad D_e = \frac{\delta_1^2/\eta + D_a + D_b}{\theta_a + \theta_b} \quad \text{for } t >> \frac{\theta_a \theta_b \eta}{(\theta_a + \theta_b)} \ .$$

The solution will yield the effective solute motion. If extra detail is required, the distance between the solute pulses in the two pore sets can be determined as

$$\delta_1 = t_e \left(\frac{v_a}{\theta_a} - \frac{v_b}{\theta_b} \right) \ . \tag{44}$$

When δ_1 is written in this form, it is shown to be the product of the equilibrium time and the difference between the two averaged microscopic velocities.

The applicability of the results obtained in this paper are dependent upon the acceptance of the assumptions implied by Equation 21. The linear form of the coupling term is shown not to be acceptable when considering very early time behavior (Dykhuizen, 1990). However, this lower limit on time will typically be significantly less than the equilibrium time constant presented here.

The choice of a constant diffusion/dispersion coefficient always generates controversy, especially if the medium is considered heterogeneous. This constant diffusion/dispersion assumption is often acceptable when considering asymptotic solutions. In this case, the dispersion is often modeled to approach a constant limiting value (de Marsily, 1986).

Finally, for the asymptotic solution to have any meaning, the transient to be modeled has to last longer than the equilibrium time, and the medium has to be larger than δ_1. This distance is often very large when considering a fractured media application.

4.3 Verification of the Moment Analysis

To quantify the errors involved in the approximation, the effective equation solution is compared to a solution of the actual dual porosity model. It is important that the comparison be made between analytical solutions for each model. In this way there is no concern about errors introduced from a numerical solution. Numerical diffusion can be significant in the solution of solute transport models, and the dispersion of the solute is of great interest.

A solution for solute transport in a simple dual velocity system is presented here. This dual velocity system has a zero convective velocity for one of the subsystems and ignores any diffusion-dispersion within either of the subsystems. Thus, the result presents a simple test for the effective dispersion caused by the coupling term. The governing equations (Equation set 21) are rewritten here for this application as

$$\theta_a \frac{\partial C_a}{\partial t} + v_a \frac{\partial C_a}{\partial z} = \frac{(C_b - C_a)}{\eta} \quad \text{, and} \tag{45}$$

$$\theta_b \frac{\partial C_b}{\partial t} = \frac{(C_a - C_b)}{\eta} \quad . \tag{46}$$

These equations can be non-dimensionalized by introducing the following variables:

$$\tau = \frac{t}{\eta \theta_b} - \frac{z \theta_a}{v_a \theta_b \eta} \quad \text{, and} \tag{47}$$

$$\beta = \frac{z}{v_a \eta} \quad . \tag{48}$$

This results in the same non-dimensional equations as obtained by Pigford, *et al.* (1980),

$$\frac{\partial C_a}{\partial \beta} = C_b - C_a \quad \text{, and} \tag{49}$$

$$\frac{\partial C_b}{\partial \tau} = C_a - C_b \quad . \tag{50}$$

Pigford, *et al.* were able to solve the equations using Laplace transforms for the following initial and boundary conditions:

$$C_a(\beta, 0) = C_b(\beta, 0) = 0 \qquad 0 \leq \beta \leq \infty \text{ , and} \tag{51}$$

$$C_a(0,\tau) = \delta(\tau) \qquad \tau \geq 0 \ , \tag{52}$$

where $\delta(\tau)$ is the Dirac delta function. This results in:

$$C_a(\beta,\tau) = \left[2\beta \ exp\ (-\tau-\beta)\frac{I_1\left(\sqrt{4\tau\beta}\right)}{\sqrt{4\tau\beta}} + \delta(\tau)\ exp\ (-\tau-\beta)\right] h(\tau) \ , \tag{53}$$

where $h(\tau)$ is the step function,

$$\begin{aligned} h(\tau) &= 1 \qquad \tau \geq 0 \ , \\ h(\tau) &= 0 \qquad \tau < 0 \ , \end{aligned} \tag{54}$$

and I_1 is the modified Bessel function of the first kind and of order 1.

It will be instructive to comment on the meaning of the above solution. First, a large spike enters the domain at the origin. This spike travels with the fracture velocity on the characteristic $\tau = 0$. The amount of solute in the spike decreases with time due to the coupling with the b subsystem. The second term in Equation 53 represents the motion of this spike. As can be seen, when this spike passes location β, it is decreased in amplitude by $exp\ (-\beta)$.

For large values of time the solution in the traveling spike has negligible concentration; the first term in the solution represents the majority of the solute in the flowing subsystem. This wave travels on the characteristic $\tau = \beta$. This translates to a dimensional velocity of

$$V_e = \frac{v_a}{\theta_a + \theta_b} \ , \tag{55}$$

which is consistent with the result from the previous sections.

In order to compare the dispersion that results from the coupling between the two subsystems, an analytic solution for the effective model is needed. The solution of Equation 43 for an initial delta function of solute at the origin is given as

$$C(z,t) = \frac{M/\theta_e}{(4\pi D_e t)^{1/2}}\ exp\ \left(-\frac{(z-V_e t)^2}{4D_e t}\right) \ , \tag{56}$$

where $$M = \int_{-\infty}^{\infty} \theta_e C(z,t)dz \ . \tag{57}$$

To compare this solution to Pigford's, M and θ_e need to be evaluated. The effective moisture content is obtained from a simple examination of Equations 1 and 2 as

$$\theta_e = \theta_a + \theta_b \ . \tag{58}$$

The value of M can be obtained from the boundary condition in the Pigford solution:

$$M = \int_{-\infty}^{\infty} C_{ao} v_a dt = \int_{-\infty}^{\infty} C_{ao} v_a d\tau \left(\frac{dt}{d\tau}\right) = v_a \theta_b \eta \ . \tag{59}$$

Thus, if we introduce the following non-dimensional variables,

$$\gamma = \frac{t}{\theta_b \eta} \ , \tag{60}$$

$$\beta = \frac{z}{v_a \eta} \ , \text{and} \tag{61}$$

$$\alpha = \frac{\theta_a}{\theta_b} \ , \tag{62}$$

the effective model solution becomes:

$$C = \frac{1}{\sqrt{4\pi\gamma/(1+\alpha)}} \ exp\left(\frac{-(\beta - \gamma/(1+\alpha))^2}{4\gamma/(1+\alpha)^3}\right) \ . \tag{63}$$

The concern here is how these two profiles compare for various times (γ), positions (β), and porosity ratios (α). To investigate this, two new variables are presented. A position variable, y, is defined as

$$y = \frac{\beta - \gamma/(1+\alpha)}{\sqrt{2\gamma/(1+\alpha)^3}} \ . \tag{64}$$

As can be seen from Equation 63, this position will be at the peak of the traveling wave (in the effective model) at all times.

The concentration is renormalized by

$$C_N = C\sqrt{2\gamma/(1+\alpha)} \ . \tag{65}$$

In using these new variables, it is easily shown that the effective solution results in the normal distribution

$$C_N = \frac{1}{\sqrt{2\pi}} \, exp \left(\frac{-y^2}{2} \right) \quad . \tag{66}$$

The two solutions can be shown to be equivalent by plotting them for various values of the variables and parameters. The approximate solution is presented in Figures 4 and 5 by plotting C_N versus y. The Pigford solution (Equation 53) is also plotted for various values of non-dimensionalized time (γ).

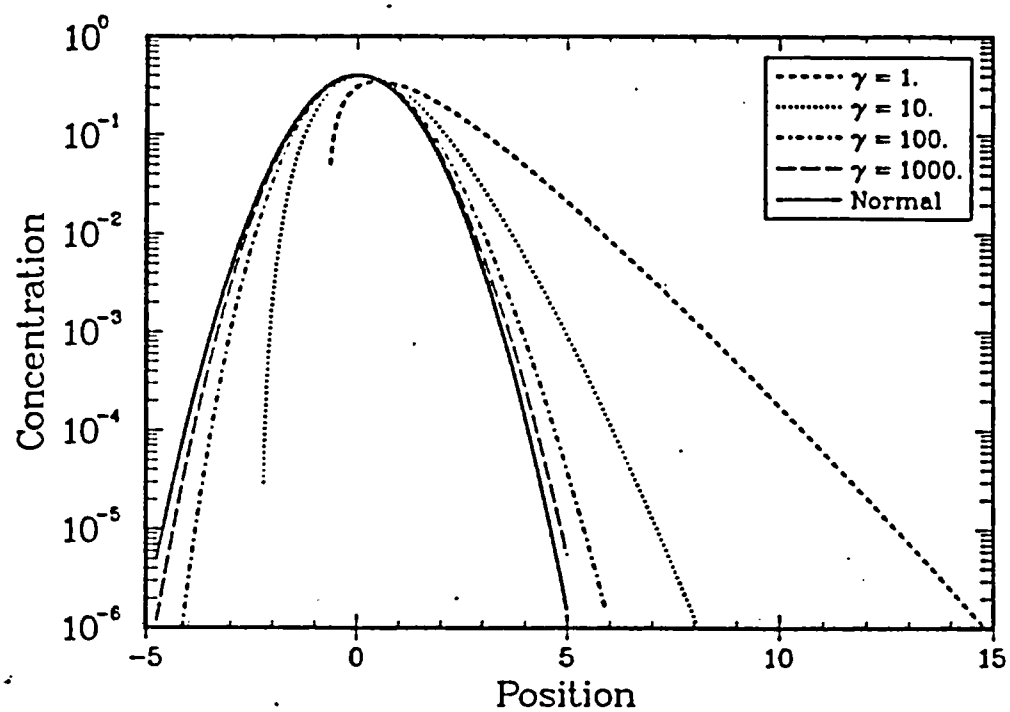

Figure 4. Non-dimensionalized comparisons between the dual porosity model at various times (γ) and effective single porosity model (normal distribution) of solute transport for $\alpha = 0.001$.

It is seen that as time increases, the Pigford solution asymptotically approaches the effective solution provided by Equation 66.

The character of the two solutions is quite different at early times. The effective model solution comes from a diffusive equation with a domain of all values of position, from plus to minus infinity, while the Pigford solution is valid only for $\beta > 0$ and $\tau > 0$. These limits result from the convective nature of the Pigford model. Solute cannot convect upstream, and cannot convect downstream faster than the fastest velocity. However,

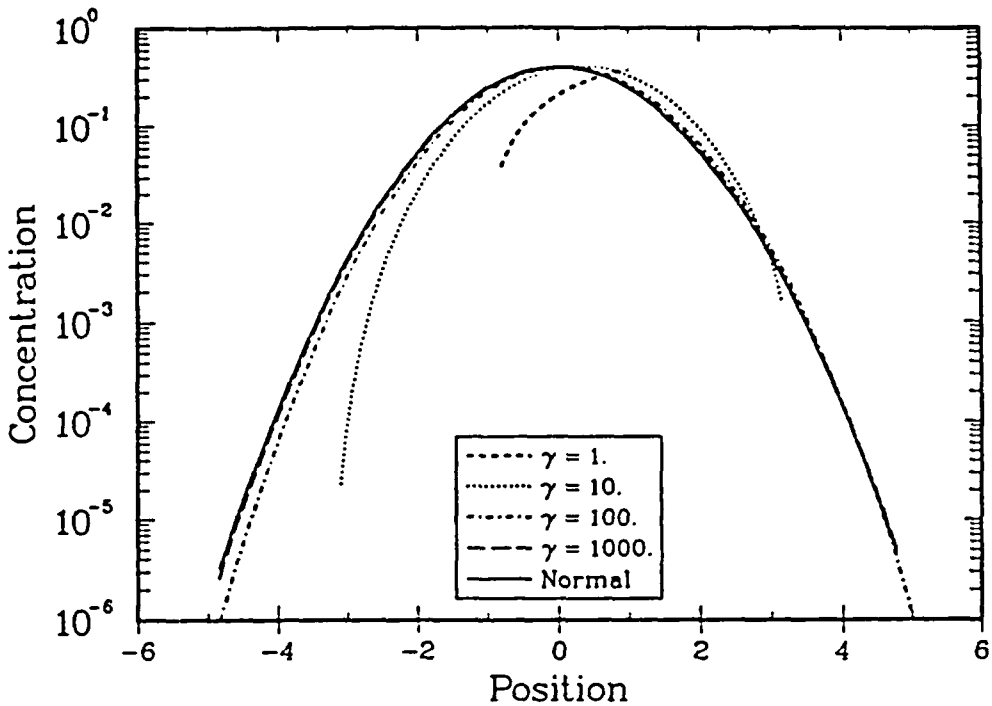

Figure 5. Non-dimensionalized comparisons between the dual porosity model for various times (γ) and effective single porosity model (normal distribution) of solute transport for $\alpha = 1.0$.

after long times (large γ), the two solutions converge for significant values of concentration. Note that the non-dimensional time (γ) can be expressed in terms of the equilibrium time (introduced with Equation 27) as

$$\gamma = \frac{t}{t_e(1+\alpha)} \quad . \tag{67}$$

The case of $\alpha = 0.001$ corresponds to the model of a fractured porous medium. In this case, the capacitance of the non-flowing matrix pore system (θ_b) is large compared to the capacitance of the fracture system (θ_a). This result is shown in Figure 4, which shows that for early times the effective single porosity model simulates well the movement of the peak of the solute pulse. However, if one is concerned with the leading edge of the traveling pulse, much larger times are required until the two models approach each other.

The case of large α, $\alpha = 1$, corresponds to the Coats and Smith model of dead end pores. In this case, the capacitance of the two systems is comparable. The better agreement shown here is somewhat fortuitous because the first term ignored in many of the asymptotic series contains the term $\alpha - 1$.

These results indicate that the asymptotic solutions are very good. They not only predict integrated properties (*i.e.*, moments of the solution), but they also can be used to show actual solute distributions in a dual porosity medium. Expansion of the approximate and exact solutions into infinite series will also demonstrate that in the limit of large times the results are identical.

4.4 Conclusions for the Moment Analysis

Many dual porosity models are governed by the same set of partial differential equations. By investigating the temporal behavior of various moments of solutions of these transport equations, effective velocity and dispersion coefficients have been obtained. The analysis proceeds along identical lines as the Taylor-Aris result for capillary dispersion. The given asymptotic solutions are valid for large times in comparison to the time constant obtained (t_e), or for distances greater than δ_1. Early time behavior (times much less than t_e) of the solute transport can be bounded by considering only the fastest system, without any coupling to the slower system. Only for intermediate times is the complexity of a dual porosity model required.

Solute sorption was not included in the above derivations. If included, it would result in a reduced effective velocity. However, it could also result in an increased effective dispersion, causing the transport to appear more diffusive.

5 SAMPLE CALCULATIONS USING YUCCA MOUNTAIN PROPERTIES

Yucca Mountain is the potential repository site for high level nuclear wastes in the United States. It is located at the western edge of the Nevada Test Site (Montazer and Wilson, 1984). In this section the models already developed are applied using Yucca Mountain properties. Properties for the various hydrogeologic layers were obtained from Barnard and Dockery (1991).

The parameters derived in the moment analysis section of this report can be evaluated using Yucca Mountain properties. The moment analysis requires that the saturation level change very slowly over space. It is best applied to unit gradient flows. Because the actual geometry of Yucca mountain consists of many finite thickness hydrogeologic layers, unit gradients do not exist at many locations. Therefore, the local velocities required for the analysis are a function of the local saturation and the local pressure gradient. This makes presentation of the results difficult due to the requirement of multi-dimensional plots. Approximate results are presented by assuming that unit gradient flows exist at Yucca Mountain. In this way the infiltration rate uniquely determines the saturation level and the local fluid velocities in the two subsystems. The parameters are presented in Figures 6 to 9.

Figure 6 shows that the effective velocity (V_e from Equation 43) is linear with the infiltration rate. That is because the porous materials considered are nearly saturated (or completely saturated) for the range of fluxes investigated. Thus, the effective velocity is nearly equal to the infiltration divided by the total porosity of the material.

Figure 7 shows the variation of the distance the solute pulse in the fracture subsystem leads the pulse in the matrix subsystem. For low infiltrations this distance is negligible when compared to the total distance the solute has to travel to reach the water table. This plot indicates that for the fluxes considered to be applicable at Yucca Mountain a dual porosity model is not required.

Figure 8 shows the time constant obtained that is a measure of the equilibration time between the fracture and matrix pore subsystems. This time approaches a constant as the system saturates.

Figure 9 shows the effective dispersion of the total system. For infiltrations greater than 10^{-9} m/sec, the added dispersion caused by the matrix and fracture systems exhibiting different convective velocities dominates the other causes of dispersion. The dispersion becomes quadratic with the infiltration rate when the extra dispersion due to the dual system becomes dominant.

Solute transport results were calculated using the full dual porosity model. Using the nominal flow rate of 0.01 mm/yr that was proposed to exist at the Yucca Mountain site,

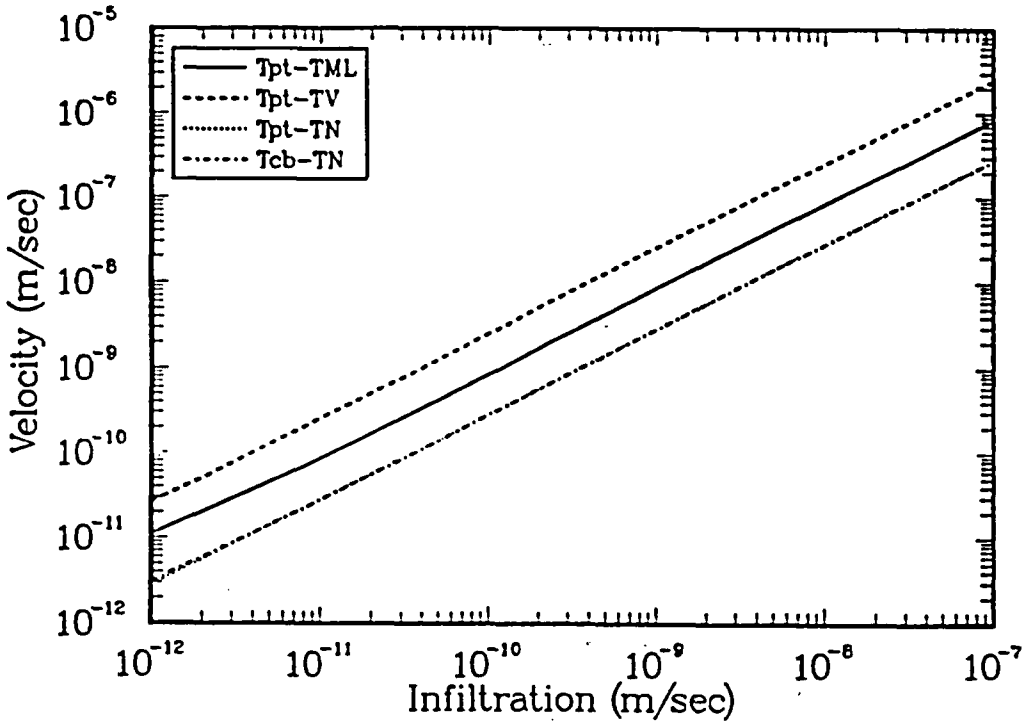

Figure 6. Effective velocity variation as a function of the infiltration rate (Tpt-TN and Tcb-TN are almost coincidental).

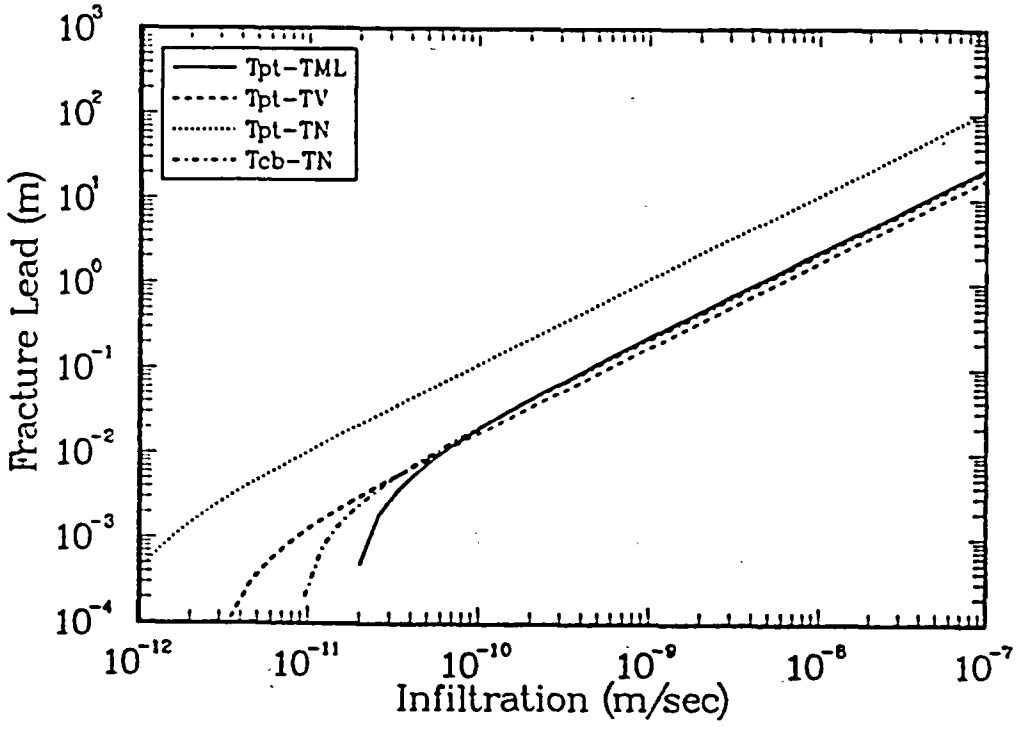

Figure 7. Distance between the fracture and matrix pore pulse locations (δ_1) as a function of the infiltration

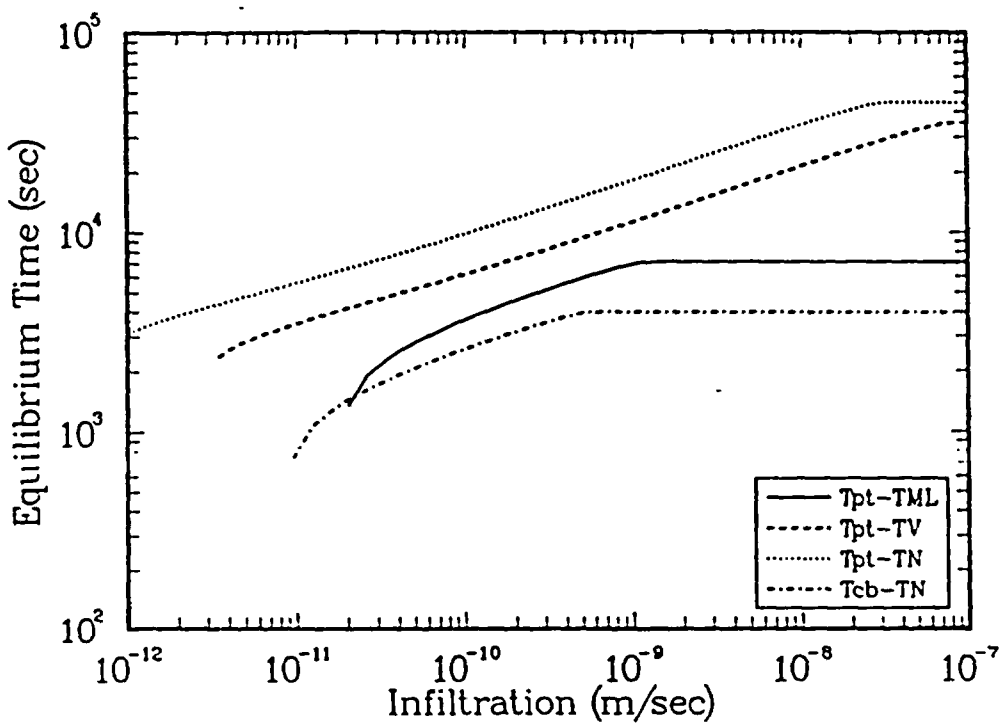

Figure 8. Equilibrium time constant as a function of the infiltration

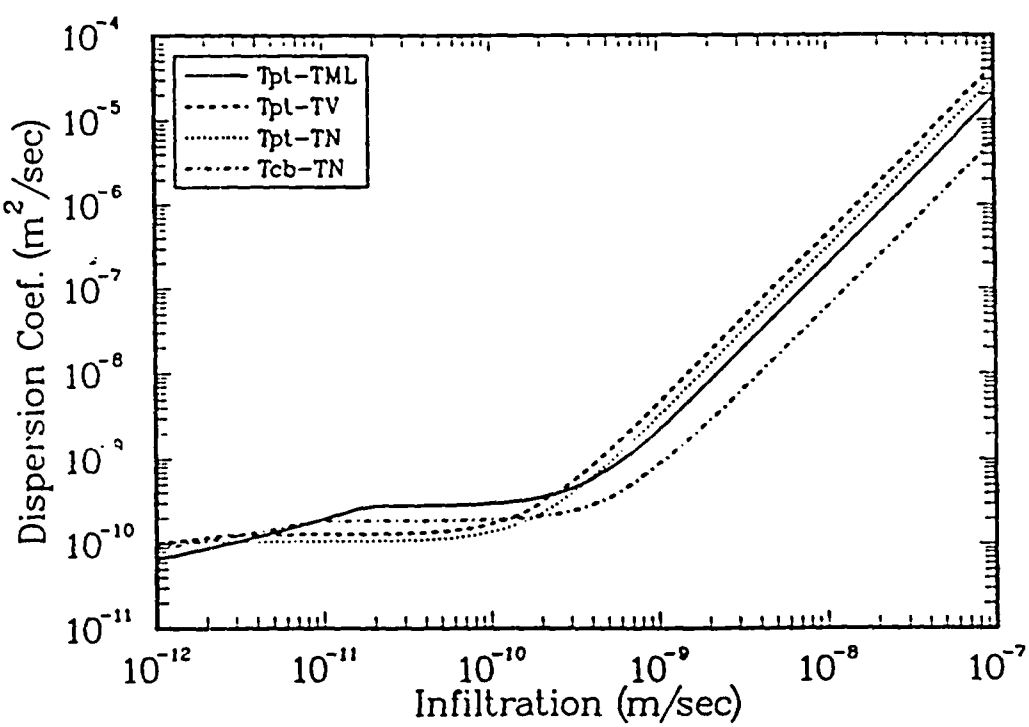

Figure 9. Effective dispersion as a function of the infiltration.

the fracture system did not transmit any flow. Therefore, the need for a dual porosity model was not demonstrated. The same results were obtained for both dual porosity and single porosity models. When the steady infiltration is increased to 0.5 mm/yr the fractures begin to flow. However, the high fracture density and the low fracture velocities result in very strong coupling between the fractures and the matrix. Again, a dual porosity model was not required to model solute transport.

Table 2 shows the parameter values used in the models. It should be noted that these parameter values are thought to be representative; however, experimental data are required to verify these choices. To solve the solute transport equation, boundary conditions have to be provided. The domain modeled was from the water table up to the repository elevation (Barnard and Dockery, 1991), using the data from drillhole G-4. A zero concentration was imposed at the lower boundary. This conservatively assumes that the water table has an infinite capacity with good mixing. A pulse of solute was injected at the upper boundary over the initial 5000 years. The solute was distributed between the fracture and matrix subsystems in proportion to their respective groundwater flow rates at the repository elevation. The flux boundary condition conservatively eliminates any diffusion of the solute upward from the repository that occurs at the low infiltrations. Figure 10 shows the distribution of Tc-99 below the repository and above the water table after 100,000 years for the infiltration rate of 0.5 mm/yr. Tc-99 is only slightly retarded by the geologic medium due to sorption reactions in layers near the repository. At the 0.5 mm/yr infiltration, the average solute particle does not reach the water table before 150,000 years. Therefore, the solute that does reach the water table is due to dispersion of the solute. On the scale of this plot, the fracture and the matrix solute concentrations are identical at any elevation. It is also shown that the assumption of a single continuum yields the same result. This is consistent with the results obtained from the moment analysis. This showed that for such a low flow rate the fracture concentration pulse will only lead the matrix pulse by less than a centimeter.

Table 2

Parameter Values Used in Transport Models

	matrix	fracture
τ_s	10	1
α	10 m	10 m
D^*	10^{-9} m ^{2}/s	10^{-9} m^2/s

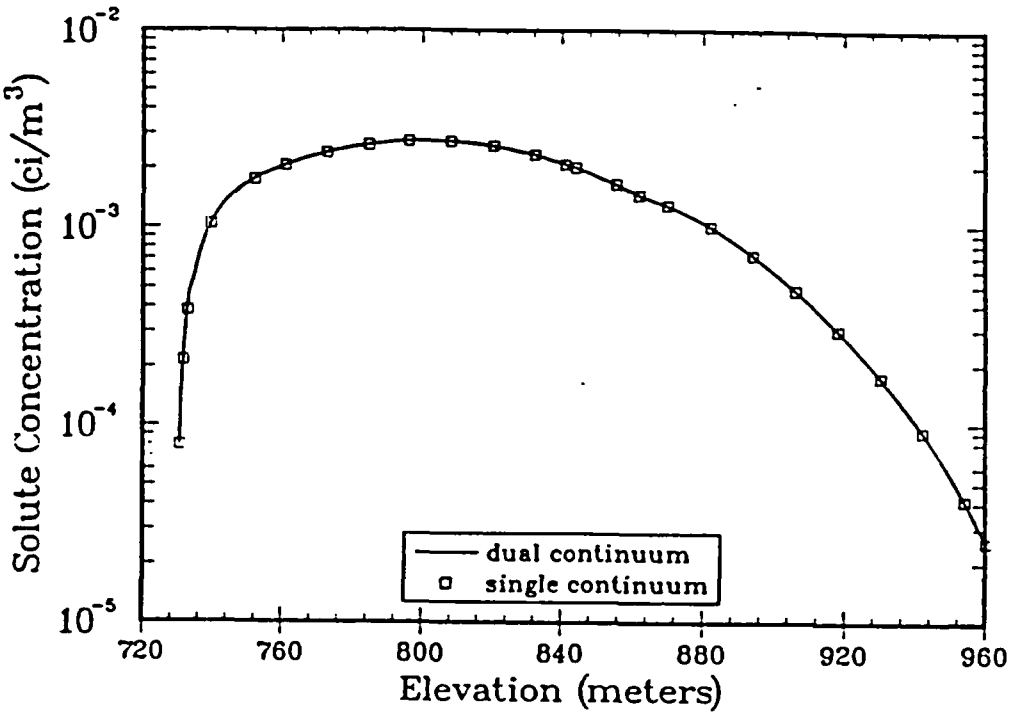

Figure 10. Solute distribution after 100,000 years of transport

The single porosity model used to obtain results for Figure 10 can be derived by two equivalent means. The first is by deleting the fracture flow system and increasing the matrix subsystem conductivity by that of the fracture subsystem. The single porosity model is also obtained by assuming an infinite coupling in the dual porosity model. The single porosity model results were verified by comparisons to simulations using the FEMTRAN (Martinez, 1985) code.

6 CONCLUSIONS

The inclusion of a dual porosity model can greatly increase the solute releases when significant fracture flow exists. This is due to the solute bypassing the water volumes in the rock matrix. However, the complexity of a dual porosity model can be avoided if one of the following situations exist for fractured system flows.

- Dry fractures. If this is the case the matrix subsystem describes the entire flow field. Fracture properties are not required. This situation occurs for fractured media at low saturations. This is considered to be the current state of the Yucca Mountain site above the water table.

- Low fracture velocity. If this case is to apply, the fracture system linear velocity is less than that of the matrix system. Only a very limited set of conditions result in a fracture system that has a measurable flow rate but a lower linear velocity than the matrix system.

- Infinite coupling. The coupling is so strong that the fracture lead distance is so small that the effective dispersion is equivalent to the sum of the two subsystem dispersion terms. If this is the case, the fracture subsystem properties still have to be incorporated into the model to allow the calculation of an effective dispersion coefficient that will be the sum of the contributions from the two subsystems.

- Flow lengths much greater than coupling lengths. This situation allows the use of the effective terms derived in the moment analysis section. For vertical flows this situation is difficult to obtain for the flow distance through each individual layer has to be at least an order of magnitude greater than the coupling length. If one is interested in the tails of the solute pulse, the layer has to be many orders of magnitude greater than the fracture lead distance (Figure 4).

- No coupling. This situation can be assumed to exist if the flow distance of interest is short when compared to the coupling length. Then only the fracture flow system needs to be included, and the matrix pore system does not participate.

It is of course desirable to eliminate the complexity of dual porosity models. The simplified models typically require only half of the computational time (or less) to obtain numerical results. Also, analytical solutions and approximations are available. For the steady flux levels considered at Yucca Mountain the dual porosity model is not required. The moment analysis results from Section 4 can be used to numerically evaluate the items listed above.

7 REFERENCES

Aris, R., 1956, "On the Dispersion of a Solute in a Fluid Flowing Through a Tube," *Proc. Roy. Soc.*, A235, 67-77. (NNA.910405.0029)

Aris, R., 1959, "On the Dispersion of a Solute by Diffusion, Convection and Exchange Between Phases," *Proc. Roy. Soc.*, A252, 538-550. (NNA.910405.0030)

Barenblatt, G. I., Iu. P. Zheltov, and I. N. Kochina, 1960, "Basic Concepts in the Theory of Seepage of Homogeneous Liquids in Fissured Rocks," *J. Applied Math and Mech.*, 24(5), 1286-1303. (NNA.870728.0027)

Barnard, R. W. and Dockery, H. A., editors, 1991, "Technical Summary of the Performance Assessment Calculational Exercise for 1990 (Pace-90) Vol. 1: 'Nominal Configuration' Hydrogeologic Parameters and Results," SAND 90-2726. (NNA.910523.0001)

Berkowitz, B., J. Bear, and C. Braester, 1988, "Continuum Models for Contaminant Transport in Fractured Porous Formulations," *Water Resour. Res.*, 24(8), 1225-1236. (NNA.910328.0076)

Burdine, T. N., 1953, "Relative Permeability Calculations from Pore Size Distribution Data," *American Institute of Mining Engineers, Petroleum Transactions*, 198, pp 71-77. (NNA.890522.0241)

Carslaw, H., and J. Jaeger, 1988, Conduction of heat in solids, Oxford Press, Oxford, UK. (NNA.900522.0259)

Casey, W. H., 1987, "Heterogeneous Kinetics and Diffusion Boundary Layers: The Example of Reaction in a Fracture," *J. Geophys. Res.*, 92, 8007-8013. (NNA.910405.0047)

Coats, K. H. and B. D. Smith, 1964, "Dead End Pore Volume and Dispersion in Porous Media," *Soc. Pet. Eng. J.*, 4, 73-84. (NNA.910523.0002)

Deans, H. H., 1963, "A Mathematical Model for Dispersion in the Direction of Flow in Porous Media," *Trans. AIME*, 228, 49-52. (NNA.910328.0075)

de Marsily, Ghislain, 1986, Quantitative Hydrogeology, Academic Press, Orlando, FL. (NNA.910207.0116)

DeSmedt, F. and P. J. Wierenga, 1984, "Solute Transfer Through Columns of Glass Beads," *Water Resour. Res.*, 20, 225-232. (NNA.910328.0077)

Dykhuizen, R. C., 1990, "A New Coupling Term for Dual Porosity Models," *Water Resour. Res.*, Vol. 26, No. 2, pp 351-356. (NNA.910328.0058)

Dykhuizen, R.C., 1987, "Transport of Solutes Through Unsaturated Fractured Media," *Water Res.*, Vol. 21, No. 12, pp 1531-1539. (NNA.890327.0047)

Eckert, E. R. G., and R. M. Drake, Jr., 1986, Analysis of Heat and Mass Transfer, McGraw–Hill, NY. (NNA.910501.0103)

Einstein, A., 1905, "On the Movement of Small Particles Suspended in a Stationary Liquid Demanded by the Molecular-Kinetic Theory of Heat," *Ann. d. Phys.*, 17 pp., 549-560. (NNA.910612.0002)

Fogden, A. F., K. A. Landman, and L. R. White, 1988, "Contaminant Transport in Fractured Porous Media: Steady State Solutions by a Boundary Integral Method," *Water Resour. Res.*, 24(8), 1384-1396. (NNA.890315.0004)

Freeze, R. A. and Cherry, 1979, J. A., Groundwater, Prentice Hall, Edgewood Cliffs, NJ. (NNA.870406.0444)

Glueckauf, E., 1955, "Theory of Chromatography Part 10: Formulae for Diffusion into Spheres and Their Application to Chromatography," *Trans. Faraday Soc.*, 51, 1540-1551. (NNA.910405.0031)

Golay, M. J. E., 1958, "Theory of Chromatography in Open and Coated Tubular Columns with Round and Rectangular Cross Sections," Gas Chromatography, D. H. Desty, editor, Butterworths, London, pp. 36-55. (NNA.910328.0068)

Goodman, T., 1964, "Application of Integral Methods to Transient Nonlinear Heat Transfer, Advances in Heat Transfer, 1, pp. 51-122, Academic Press. (NNA.891109.0116)

Grisak, G. E., and J. F. Pickens, 1980, "Solute Transport Through Fractured Media 1. The Effect of Matrix Diffusion," *Water Resour. Res.*, 16(4), 719-730. (NNA.890315.0006)

Lapidus, L. and N. R. Amundson, 1952, "Mathematics of Adsorption in Beds VI: The Effect of Longitudinal Diffusion in Ion Exchange and Chromatographic Columns," *J. Phys. Chem.*, 56, 984-988. (NNA.910405.0032)

Martinez, M. J., 1985, "FEMTRAN – A Finite Element Computer Program for Simulating Radionuclide Transport Through Porous Media", SAND84-0747, Sandia National Laboratories, Albuquerque, NM. (NNA.870728.0029)

Montazer, P., and W. E. Wilson, 1984, "Conceptual Hydrologic Model of Flow in the Unsaturated Zone, Yucca Mountain, Nevada," USGS-WRI-84-4345, U.S. Geological Survey, Lakewood, CO. (NNA.890327.0051)

Neretnieks, I. and A. Rasmuson, 1984, "An Approach to Modeling Radionuclide Migration in a Medium with Strongly Varying Velocity and Block Sizes Along the Flow Path," *Water Resour. Res.*, 20(12), 1823-1836. (NNA.910405.0022)

Parker, J. C. and A. J. Valocchi, 1986, "Constraints on the Validity of Equilibrium and First Order Kinetic Transport Models in Structured Soils," *Water Resour. Res.*, 22, 399-407. (NNA.910405.0023)

Pigford, T. H., P. L. Chambre, M. Albert, M. Foglia, M. Harada, F. Iwamoto, T. Kanki, D. Leung, S. Masuda, S. Muraoka, D. Ting, 1908, "Migration of Radionuclides through Sorbing Media, Analytical Solutions II," LBL-11616, Lawrence Berkley Laboratory. (NNA.910412.0003)

Pohlhausen, K., 1921, "Zur Näherungsweisen Intergration der Differentialgleichung der Grenzschiet," *Z. Agnew Math. Mech*, 1, 252-268. (NNA.890621.0038)

Rubin, J., 1983, "Transport of Reacting Solutes in Porous Media," *Water Resour. Res.*, 19, 1231-1252. (NNA.910405.0024)

Schlichting, J., 1968, Boundary Layer Theory, 6th Ed., McGraw-Hill, NY. (NNA.910522.0049)

Taylor, G. I., 1953, "Dispersion of Soluble Matter in Solvent Flowing Slowly Through a Tube," *Proc. Roy. Soc.*, A219, 186-203. (NNA.910405.0033)

van Genuchten, M. T., 1985, "A General Approach for Modeling Solute Transport in Structured Solis," in Hydrogeology of Rocks of Low Permeability, Proceedings of the 17th International Congress, International Association of Hydrogeologists, Tucson, AZ, 17(1), 513-526. (NNA.910327.0065)

Warren, J. E., and P. J. Root, 1963, "The Behavior of Naturally Fractured Reservoirs," *Soc. Petrol. Eng. J.*, 3(5), 245-255. (NNA.890522.0276)

Westhaver, J. W., 1942, "Theory of Open-Tube Distillation Columns," *Ind. Eng. Chem.*, 34(1), 126-130. (NNA.910405.0034)

Wilson, M. L., and A. L. Dudley, 1987, "Radionuclide Transport in an Unsaturated Fractured Medium," in *Flow and Transport Through Unsaturated Fractured Rock*, D. D. Evans and R. J. Nicholson, Eds., Geophysical Monograph 42. (HQS.880517.2907)

Zanotti, F. and R. G. Carbonell, 1984a, "Development of Transport Equations for Multiphase Systems – I," *Chem. Engr. Sci.*, 39(2), 263-278. (NNA.900123.0080)

Zanotti, F. and R. G. Carbonell, 1984b, "Development of Transport Equations for Multiphase Systems – II," *Chem. Engr. Sci.*, 39(2), 279-297. (NNA.900123.0080)

Zimmerman, R. W., and A. S. Bodvarsson, 1989, "An Approximate Solution for One-Dimensional Absorption in Unsaturated Porous Media," *Water Resour. Res.*, 25(6), 1422-1428. (NNA.910221.0144)

Appendix A. Reference Information Base

Information from the Reference Information Base Used in this Report

This report contains no information from the Reference Information Base.

Candidate Information for the Reference Information Base

This report contains no candidate information for the Reference Information Base.

Candidate Information for the Site & Engineering Properties Data Base

This report contains no candidate information for the Site and Engineering Properties Data Base.

DISTRIBUTION LIST

1 John W. Bartlett, Director (RW-1)
Office of Civilian Radioactive
Waste Management
U.S. Department of Energy
Forrestal Bldg.
Washington, D.C. 20585

1 F. G. Peters, Deputy Director (RW-2)
Office of Civilian Radioactive
Waste Management
U.S. Department of Energy
Forrestal Bldg.
Washington, D.C. 20585

1 D. G. Horton (RW-3)
Office of Quality Assurance
Office of Civilian Radioactive
Waste Management
U.S. Department of Energy
Forrestal Bldg.
Washington, D.C. 20585

1 T. H. Isaacs (RW-4)
Office of Strategic Planning
and International Programs
Office of Civilian Radioactive
Waste Management
U.S. Department of Energy
Forrestal Bldg.
Washington, D.C. 20585

1 J. D. Saltzman (RW-5)
Office of External Relations
Office of Civilian Radioactive
Waste Management
U.S. Department of Energy
Forrestal Bldg.
Washington, D.C. 20585

1 Samuel Rousso (RW-10)
Office of Program and Resources
Management
Office of Civilian Radioactive
Waste Management
U.S. Department of Energy
Forrestal Bldg.
Washington, D.C. 20585

1 Carl P. Gertz (RW-20)
Office of Geologic Disposal
Office of Civilian Radioactive
Waste Management
U.S. Department of Energy
Forrestal Bldg.
Washington, D.C. 20585

1 D. E. Shelor (RW-30)
Office of Systems and Compliance
Office of Civilian Radioactive
Waste Management
U.S. Department of Energy
Forrestal Bldg.
Washington, D.C. 20585

1 L. H. Barrett (RW-40)
Office of Storage and Transportation
Office of Civilian Radioactive
Waste Management
U.S. Department of Energy
Forrestal Bldg.
Washington, D.C. 20585

1 F. G. Peters (RW-50)
Office of Contractor Business
Management
Office of Civilian Radioactive
Waste Management
U.S. Department of Energy
Forrestal Bldg.
Washington, D.C. 20585

1 J. C. Bresee (RW-10)
Office of Civilian Radioactive
Waste Management
U.S. Department of Energy
Forrestal Bldg.
Washington, D.C. 20585

1 S. J. Brocoum (RW-20)
Office of Civilian Radioactive
Waste Management
U.S. Department of Energy
Forrestal Building
Washington, D.C. 20585

1 Gerald Parker (RW-30)
Office of Civilian Radioactive
Waste Management
U.S. Department of Energy
Forrestal Bldg.
Washington, D.C. 20585

1 D. U. Deere, Chairman
Nuclear Waste Technical
Review Board
1100 Wilson Blvd. #910
Arlington, VA 22209-2297

5 Carl P. Gertz, Project Manager
Yucca Mountain Project Office
Nevada Operations Office
U.S. Department of Energy
Mail Stop 523
P.O. Box 98518
Las Vegas, NV 89193-8518

1 C. L. West, Director
Office of External Affairs
Nevada Operations Office
U.S. Department of Energy
P.O. Box 98518
Las Vegas, NV 89193-8518

12 Technical Information Office
Nevada Operations Office
U. S. Department of Energy
P.O. Box 98518
Las Vegas, NV 89193-8518

1 P. K. Fitzsimmons, Director
Health Physics & Environmental Division
Nevada Operations Office
U.S. Department of Energy
P.O. Box 98518
Las Vegas, NV 89193-8518

1 Repository Licensing & Quality Assurance Project Directorate
Division of Waste Management
U.S. Nuclear Regulatory Commission
Washington, D.C. 20555

1 Senior Project Manager for Yucca Mountain Repository Project Branch
Division of Waste Management
U.S. Nuclear Regulatory Commission
Washington, D.C. 20555

1 NRC Document Control Desk
Division of Waste Management
U.S. Nuclear Regulatory Commission
Washington, D.C. 20555

1 E. P. Binnall
Field Systems Group Leader
Building 50B/4235
Lawrence Berkeley Laboratory
Berkeley, CA 94720

1 Center for Nuclear Waste Regulatory Analyses
6220 Culebra Road
Drawer 28510
San Antonio, TX 78284

3 L. J. Jardine
Technical Project Officer for YMP
Lawrence Livermore National Laboratory
Mail Stop L-204
P.O. Box 808
Livermore, CA 94550

4 R. J. Herbst
Technical Project Officer for YMP
Los Alamos National Laboratory
N-5, Mail Stop J521
P.O. Box 1663
Los Alamos, NM 87545

1 H. N. Kalia
Exploratory Shaft Test Manager
Los Alamos National Laboratory
Mail Stop 527
101 Convention Center Dr.
Suite 820
Las Vegas, NV 89109

1 J. F. Divine
Assistant Director for Engineering Geology
U.S. Geological Survey
106 National Center
12201 Sunrise Valley Dr.
Reston, VA 22092

6 L. R. Hayes
Technical Project Officer for YMP
U.S. Geological Survey
P.O. Box 25046
421 Federal Center
Denver, CO 80225

1 D. Zesiger
U.S. Geological Survey
101 Convention Center Dr.
Suite 860 - MS509
Las Vegas, NV 89109

1 DeWayne A. Campbell
YMP Technical Project Officer
Bureau of Reclamation
P.O. Box 25007 Bldg. 67
Denver, CO 80225-0007

1 K. W. Causseaux
NHP Reports Chief
U.S. Geological Survey
P.O. Box 25046
421 Federal Center
Denver, CO 80225

1 R. V. Watkins, Chief
Project Planning and Management
U.S. Geological Survey
P.O. Box 25046
421 Federal Center
Denver, CO 80225

1 V. M. Glanzman
U.S. Geological Survey
P.O. Box 25046
913 Federal Center
Denver, CO 80225

1 J. H. Nelson
Technical Project Officer for YMP
Science Applications International Corp.
101 Convention Center Dr.
Suite 407
Las Vegas, NV 89109

2 SAIC-T&MSS Library
Science Applications International Corp.
101 Convention Center Dr.
Suite 407
Las Vegas, NV 89109

1 Elaine Ezra
YMP GIS Project Manager
EG&G Energy Measurements, Inc.
Mail Stop D-12
P.O. Box 1912
Las Vegas, NV 89125

1 W. M. Hewitt, Program Manager
Roy F. Weston, Inc.
955 L'Enfant Plaza, Southwest
Suite 800
Washington, D.C. 20024

1 Technical Information Center
Roy F. Weston, Inc.
955 L'Enfant Plaza, Southwest
Suite 800
Washington, D.C. 20024

1 D. L. Fraser, General Manager
Reynolds Electrical & Engineering Co.
P.O. Box 98521
Mail Stop 555
Las Vegas, NV 89193-8521

1 Robert F. Pritchett
Technical Project Officer for YMP
Reynolds Electrical & Engineering Co.
Mail Stop 615
P.O. Box 98521
Las Vegas, NV 89193-8521

1 A. E. Gurrola
General Manager
Raytheon, Inc.
Mail Stop 580
P.O. Box 93838
Las Vegas, NV 89193-3838

1 James C. Calovini
Raytheon Services, Inc.
101 Convention Center Dr.
Suite P-280
Las Vegas, NV 89109

1 D. L. Lockwood, General Manager
Raytheon Services, Inc.
Mail Stop 514
P.O. Box 93265
Las Vegas, NV 89193-3265

1 Richard L. Bullock
Technical Project Officer for YMP
Raytheon Services, Inc.
101 Convention Center Dr.
Suite P250
Las Vegas, NV 89109

1 R. E. Lowder
Technical Project Officer for YMP
MAC Technical Services
Valley Bank Center
101 Convention Center Drive
Suite 1100
Las Vegas, NV 89109

1 D. J. Bales
Science and Technology Division
Office of Scientific and Technical Information
U.S. Department of Energy
P.O. Box 62
Oak Ridge, TN 37831

1 Carlos G. Bell, Jr.
Professor of Civil Engineering
Civil and Mechanical Engineering Department
University of Nevada, Las Vegas
4505 South Maryland Parkway
Las Vegas, NV 89154

1 C. F. Costa, Director
Nuclear Radiation Assessment Division
U.S. Environmental Protection Agency
Environmental Monitoring Systems Laboratory
P.O. Box 93478
Las Vegas, NV 89193-3478

1 ONWI Library
Battelle Columbus Laboratory
Office of Nuclear Waste Isolation
505 King Avenue
Columbus, OH 43201

1 T. Hay, Executive Assistant
Office of the Governor
State of Nevada
Capitol Complex
Carson City, NV 89710

3 R. R. Loux, Jr.
Executive Director
Nuclear Waste Project Office
State of Nevada
Evergreen Center, Suite 252
1802 North Carson Street
Carson City, NV 89710

1 C. H. Johnson
Technical Program Manager
Nuclear Waste Project Office
State of Nevada
Evergreen Center, Suite 252
1802 North Carson Street
Carson City, NV 89710

1 John Fordham
Water Resources Center
Desert Research Institute
P.O. Box 60220
Reno, NV 89506

1 Dr. Martin Mifflin
Desert Research Institute
Water Resources Center
2505 Chandler Avenue
Suite 1
Las Vegas, NV 89120

1 Eric Anderson
Mountain West Research-Southwest Inc.
2901 N. Central Ave. #1000
Phoenix, AZ 85012-2730

1 Department of Comprehensive Planning
Clark County
225 Bridger Avenue, 7th Floor
Las Vegas, NV 89155

1 Planning Department
Nye County
P.O. Box 153
Tonopah, NV 89049

1 Lincoln County Commission
Lincoln County
P.O. Box 90
Pioche, NV 89043

5 Judy Foremaster
City of Caliente
P.O. Box 158
Caliente, NV 89008

1 Economic Development Department
City of Las Vegas
400 East Stewart Avenue
Las Vegas, NV 89109

1 Community Planning & Development
City of North Las Vegas
P.O. Box 4086
North Las Vegas, NV 89030

1 Director of Community Planning
City of Boulder City
P.O. Box 367
Boulder City, NV 89005

1 Commission of the European
Communities
200 Rue de la Loi
B-1049 Brussels
Belgium

1	6300	T. O. Hunter, Actg.
1	6310	T. E. Blejwas, Actg.
1	6310A	L. E. Shephard
1	6311	A. L. Stevens
1	6312	F. W. Bingham
1	6312	R. W. Barnard
1	6312	E. Dunn
1	6312	P. G. Kaplan
1	6312	M. L. Wilson
1	6313	L. S. Costin
1	6315	F. B. Nimick, Actg.
1	6316	R. P. Sandoval
1	6317	S. Sinnock
2	6318	L. J. Erickson for 100/12141/SAND90-2619/NQ
1	6318	C. Crawford for Accession No. Data Base
1	6319	R. R. Richards
1	1510	J. C. Cummings
1	1511	J. S. Rottler
1	1513	R. D. Skocypec
5	1513	R. C. Dykhuizen
5	3141	S. A. Landenberger
8	3145	Document Processing for DOE/OSTI
3	3151	G. C. Claycomb
20	6341	WMT Library
1	6410	D. J. McCloskey, Actg.
1	8523	Technical Library

The number in the lower right-hand corner is an accession number used for Office of Civilian Radioactive Waste Management purposes only. It should not be used when ordering this publication.

NNA.910612.0001

Org.	Bldg	Name	Rec'd by	Org.	Bldg	Name	Rec'd by

Sandia National Laboratories